SCIPP 98/18
1998

The Kalman Filter Technique applied to Track Fitting in GLAST

Jose A. Hernando

Santa Cruz Institute for Particle Physics
University of California, Santa Cruz

Using the iterative property of the Kalman Filter technique an estimate of the track parameter resolution for the case of the GLAST design (straight line tracks and periodic hits measurements) has been computed at the vertex position.

1 Introduction

The GLAST experiment [1] will locate the high energy gamma ray sources in the Universe via the reconstruction of the gamma directions that arrive at Earth. This direction is measured *via* the conversion of the gamma in thin lead planes and the subsequent reconstruction of the electron/positron pair with a precise tracker, and the measurement of the energy with a calorimeter. The converter, needed to produce the interactions, introduces however, an unavoidable error due to the multiple Coulomb scattering (MS) in the trajectory of the particles. It is crucial to understand how does the multiple scattering affect the reconstruction of the particle trajectories.

The presence of non-negligible multiple scattering complicates the fitting procedure and the pattern recognition problem. The covariance matrix becomes non-diagonal in order to take into account the error correlation between different planes; thus it becomes larger and requires more computing time to invert it. The Kalman Filter (KF) technique aliviates both problems in a simple and nice way. This method was introduced by Kalman [2], and was first applied to High Energy Physics in the eightys by Frühwirth [3] and Billoir (who re-invented it [4]) and it has become a common technique in present experiments. The convenience of the Kalman Filter to the track fitting problem when multiple scattering errors are involved, comes from its iterative property. KF considers only one measurement each time, introducing it independently into the fit. This property allows to handle in a nice way the decision of adding or removing a given measurement to the track, therefore aiding the track finding. It also permits the introduction of *random errors* (as it is the case of the multiple scattering) in a natural way. Now, one has to consider only the multiple scattering error produced between two measurement planes. This simplifies greatly the problem of the MS error.

The KF also allows us to compute the precision or resolution on the track parameters at the vertex position, since it provides the parameters and the covariance matrices of the track at each measurement location, most importantly, at the first plane. Extrapolating this covariance matrix to the interaction vertex, one obtains the resolution of the track parameters. With this technique one can quantify the multiple scattering effect, and the relation with the other detector parameters. For example, on can address the following question: "when does a given multiple scattering error make useless the inclusion of a new measurement into the fit?". In other words, "how many planes are relevant in the fit for a given multiple scattering error?".

For the case of GLAST, the track model is a straight line and the measurements are a set of periodic hit positions. The distance between planes, the resolution and the amount of MS per plane, are constant. This makes the application of the KF simple and straight forward. In this note the calculation of the track parameter resolution at the vertex is computed for this case. Despite its simplicity, the results can be apply to real experiment, like GLAST in Astro Physics or NOMAD-STAR [6] in High Energy Physics. It turns out that a dimensionless parameterization is possible that uses only two parameters: the number of planes N in the tracker, and the ratio between the multiple scattering error and the nominal resolution slope $f_{ms} = \frac{\theta_0}{\theta_n}$, (where θ_0 is the multiple scattering error in the slope introduced between two planes and $\theta_n = \frac{\sigma}{d}$ is the *nominal resolution* - σ is the spatial hit resolution and d is the distance between two measurement planes-). The parameter resolution is then presented as a dimensionless factor (called the *improving factor*) f_i with respect the *nominal resolution*, for example, the track slope resolution is given by: $\sigma_\theta = f_\theta(N, f_{ms}) \times \theta_n$. This dimensionless parameterization addresses the problem in a general way.

This calculation makes several approximations, such as the assumption of a Gaussian distribution of the MS (ignoring the important non-Gaussian tails) or neglecting the effects of the recoil of the nucleus. There are other instrumental problems not considered here, like the pattern recognition, inefficiencies, and dead areas, or the energy matching between the track and the calorimeter. However, this calculation should provide a quantitative estimation of how the MS affects the precision of the detector.

This note is organized as follows: in the second section a quick review of the Kalman Filter is presented (for an introduction the reader can follow historic references by Frühwirth [3] or the report by B. Jones [5]). The calculation of the parameter resolution for a straight line and periodic measurements is given in section three. And the application to GLAST is disccused in the last section.

2 Brief summary of the Kalman Filter

2.1 Some general considerations about the Kalman Filter

The KF is an iterative process. When it incorporates a new measurement the track parameters are recomputed. This property is very useful when dealing with *random errors* (such as the MS) introduced between every pair of measurements.

The KF is based on the linear square estimator. For every plane, it minimizes the residuals with respect to their errors: $[\vec{m} - \vec{f}(\vec{p})]^T \mathbf{W} [\vec{m} - \vec{f}(\vec{p})]$, where $\vec{m}$ is the measurements at the plane, $\vec{p}$ is the track parameters, $f(\vec{p})$ is the track model and $\mathbf{W}$ is the positive weight matrix, that takes into account errors in the plane. Through $\mathbf{W}$ the KF handles the random errors. The two components of $\mathbf{W}$ are: the detector resolution weight matrix $\mathbf{G}$, and second, the extrapolation errors, that include, the MS matrix $\mathbf{Q}$. If the errors are Gaussian the least square estimator gives the *optimal* parameters. In this case, the χ^2 per degree of freedom, as it is well known, validates the initial hypothesis and the understanding of the errors. For the KF, there is a second quantity that can be used to test the fit, this is the pull of the parameters, defined as the residual between the measurements and the final fitted parameters, divided by the errors, these normalize residuals should be Gaussianly distributed with a standard deviation equal to the unity.

The KF assumes that the system is linear, that is, that the track model between two measurement planes is linear in the parameters (in general the approximation to the first term (linear) of a the Taylor series is valid). If the system is linear and the error are Gaussian the Filter is *efficient*, in other words, no other non-linear estimator could do better.

2.2 Implementation of the Kalman Filter

The KF is divided in two steps, called the *filter* and the *smoother*. In the *filter* process the measurements further along the track are introduced in the fit and the parameters are computed at the new (added) plane; in the *smoother*, the correction of the parameters are transported backwards from the last plane to the initial one, and the final parameters are obtained. It is important to distinguish clearly the three terms, called *projected, fitted*, and *smoothed*.

The *filter* starts from the first plane with a reasonable guess of the parameters $\vec{p}_0$ and a large covariance matrix that reflects our ignorance of the initial parameters $\mathbf{C}_0$. It incorporates measurement by measurement, computing the parameters (called *fitted*) at every new plane. From the *fitted* parameters $\vec{p}_k$ and covariances $\mathbf{C}_k$ at a given plane k, one computes first, the *projected* parameters $\vec{p}_{k,proj}$ at the next plane $(k+1)$, using a *linear* extrapolation, via the transport matrix $\mathbf{F}$ (first term in a Taylor series $F_{ij} = \frac{\partial p_{k+1,projec,j}}{\partial p_{k,i}}$). The random errors (i.e. multiple scattering) are introduced into the *projected covariance* matrix, adding the random error covariance matrix $(\mathbf{Q})$ to the extrapolated covariance matrix $(\mathbf{F^T C_k F})$. The *projected* objects are:

$$\begin{aligned} \vec{p}_{k+1,proj} &= \mathbf{F}_k \vec{p}_k \\ \mathbf{C}_{k+1,proj} &= \mathbf{F}_k \mathbf{C}_k \mathbf{F}_k^T + \mathbf{Q}_k \end{aligned} \tag{1}$$

In the next plane $(k+1)$, one has two quantities: the *projected* objects and the *measurements* (note that the conversion of the measurement to the parameters is via a linear matrix $\mathbf{H}$, in this sense, the residual are denoted with $\vec{m} - \mathbf{H}\vec{p}$). Both “measure” the same objects, so the *fitted* parameter vector and covariance matrix are obtained by *weighting* the *projected* ones and the *measurements* at the new plane. The *filter* quantities are:

$$\begin{aligned} \vec{p}_{k+1} &= \mathbf{C}_{k+1}\, [\mathbf{C}^{-1}_{k+1,proj} \vec{p}_{k+1,proj} + \mathbf{H}_k^T \mathbf{G}_{k+1} \vec{m}\ ] \\ \mathbf{C}_{k+1} &= [\mathbf{C}^{-1}_{k+1,proj} + \mathbf{H}^T \mathbf{G} \mathbf{H}]^{-1} \end{aligned} \tag{2}$$

At this point, the information further along the track does not influence the preceding measurements, that is planes k' where $k' < k$ do not receive information for the measurement at the k^{th} plane. The smoother is going to propagate this information, and correct the previous planes with the measurements of the posterior planes. The job is done by a backward transport matrix $\mathbf{A_k}$. This is the normal back transport matrix $\mathbf{F^T}$ weighted with the (previous) covariance $\mathbf{C}_k$ at the plane k and the (posterior) *projected* covariance $\mathbf{C}_{k+1,proj}$ at the plane $k+1$ (note that this one includes the “random” errors). This weight acts as expected, reducing the correction when the “random” errors are large. The *smoother* or final parameters $\vec{p}_{k,smooth}$ and covariances $\mathbf{C}_{k,smooth}$, are computed transporting back the corrections between *smoothed* and *projected* objects. The back-transportation matrix is:

$$\mathbf{A}_k = \mathbf{C}_k \mathbf{F}_k^T \mathbf{C}^{-1}_{k+1,proj} \tag{3}$$

The *smoother* parameter vector and covariance matrix are:

$$\begin{aligned} \vec{p}_{k,smooth} &= \vec{p}_k + \mathbf{A}_k(\vec{p}_{k+1,smooth} - \vec{p}_{k+1,proj}) \\ \mathbf{C}_{k,smooth} &= \mathbf{C}_k + \mathbf{A}_k(\mathbf{C}_{k+1,smooth} - \mathbf{C}_{k+1,proj})\mathbf{A}_k^T \end{aligned} \tag{4}$$

At this stage the Filter provides the final *smoothed* parameters and covariances.

3 Track parameter errors for a straight line

In this section, we apply the Kalman Filter to the case where the trajectory is a straight line, and the tracker device measures a discrete set of periodic hit positions. In addition, we compute the covariance matrix at the interaction vertex.

3.1 The relevant parameters

The tracker device has several identical modules, one after the other, composed by a passive material plane (converter) -where the interactions take place-, followed by a measuring plane (for example silicon planes). We assume that the tracker only measures the hit positions at every plane. The spatial resolution, the distance between planes, and the thickness of the converter are constant. That simplifies that application of the Kalman Filter. The "random" error is the multiple scattering introduced by the material. We consider that the converter is just in front of the measuring plane to reduce the MS error in the propagation between the two surfaces.

There are two kinds of parameters. The tracker properties can be described by:

1. σ the spatial resolution of the measurement planes,
2. d the distance between two measurement planes (they are equally spaced),
3. N the number of planes,
4. $x_0 = z/X_0$ the fraction of radiation length of the passive material (where z is the thickness of the material and X_0 is the radiation length).

And the particle parameters by:

1. E the particle energy.
2. θ the incident angle.

σ and d represent the granularity of the device, the precision of a single module, (we will call σ and $\theta_n = \frac{\sigma}{d}$ the *nominal resolutions*); they are chosen to meet the physics goals of the experiment. The tracker precision depends on the number of planes N, but this dependence it strongly reduced by the presence of the multiple scattering. The number of planes is a delicate issue. It depends on the thickness of the converter per module and the total radiation length needed for the experiment. The MS error ($\theta_0 = \frac{k}{\beta\, p}\sqrt{x_0}\ (1 + 0.038\ \ln x_0)$) affects the track slope and depends on the x_0 and the energy E of the particle, (here $k = 0.015$ GeV, β is the Lorenz factor, and p is the particle momentum). θ_0 imposes a limit in the tracker resolution. Each experiment has different requirements, and the value of θ_0, and therefore x_0, has a maximum tolerable value to achieve the physics goal. This maximum must be calculated with the complete tracker, and will also depend on the rest of the parameters: the granularity and the number of planes N. The thickness of the converter z can vary from a thin foil to the total gap when the material is uniformed distributed between the two measurement planes. In this section we examine the two extreme cases $z = 0$ and $z = d$, experiments like GLAST want the track slope resolution to be kept as small as possible, then a small converted thickness is desirable, but experiments like NOMAD-STAR where the main interest is the extrapolation of the track to the vertex, a reasonable distance between the interaction and the first measurement is needed to separate the tracks, and therefore the second option is preferred.

3.2 Elements of the Kalman Filter for the straight line case

Let specify the ingredients of the Kalman Filter (the vectors and matrices) for our particular case. The track parameters are:

$$\vec{p} = \begin{pmatrix} x \\ \tan\theta \end{pmatrix}_k \tag{5}$$

Where x is the coordinate position and $\tan\theta$ is the projected track slope at plane k (we consider first the case of perpendicular tracks that allows to use the approximation of $\tan\theta \simeq \theta$, and we will discuss later the dependence with the incident angle).

The extrapolation matrix $\mathbf{F}$ is *linear*:

$$\mathbf{F} = \begin{pmatrix} 1 & d \\ 0 & 1 \end{pmatrix} \tag{6}$$

The measurement planes provides the hit positions, so the the weight matrix $\mathbf{G}$ and the measurement matrix $\mathbf{H}$ are also linear:

$$\mathbf{G} = \begin{pmatrix} 1/\sigma^2 & 0 \\ 0 & 0 \end{pmatrix} \quad \mathbf{H} = \begin{pmatrix} 1 & 0 \\ 0 & 0 \end{pmatrix} \tag{7}$$

The multiple scattering covariance matrix $\mathbf{Q}$ is

$$\mathbf{Q} = \begin{pmatrix} \theta_0^2 z^2/3 & \theta_0^2 z/2 \\ \theta_0^2 z/2 & \theta_0^2 \end{pmatrix} \tag{8}$$

and can be derived from:

$$Q_{ij} = \int_0^s \frac{\partial p_i}{\partial \theta_0} \frac{\partial p_j}{\partial \theta_0} \quad \frac{\partial \theta_0^2}{\partial s} ds \tag{9}$$

Which gives the propagation of multiple scattering angle error to the track parameters integrated along the particle path. Here $\frac{\partial \vec{p}}{\partial \theta_0}$ is the variation of the track parameters with respect the multiple scattering angle, $\frac{\partial\theta_0^2}{\partial s}$ is the error introduced per unit length, and s is the particle trajectory. In the case of the straight line track, where z is the forward direction, the above simplifies to:

$$\frac{\partial x}{\partial\theta_0} = z\frac{\partial\tan\theta}{\partial\theta_0} = \frac{z}{\cos^2\theta}; \quad \frac{\partial\tan\theta}{\partial\theta_0} = \frac{1}{\cos^2\theta}; \quad \frac{\partial\theta_0^2}{\partial s} = (\frac{k}{\beta p})^2\frac{1}{X_0}; \; ds = \frac{dz}{\cos\theta} \tag{10}$$

Where $k = 0.015$ GeV, β is the Lorenz factor and p is the momentum of the particle, $\frac{\partial\theta_0^2}{\partial s}$ is just a constant. For perpendicular tracks $\tan\theta \simeq \theta$ we recuperate the matrix above, and for other incident angle, the dependence of the multiple scattering covariance elements are proportional to $1/\cos^5\theta$ (we will come back later to this point).

3.3 The asymptotic limits

The tracker precision can be computed in a simple way, without using the Kalman Filter, in the case when the multiple scattering is large with respect the nominal resolution (i.e. $\theta_0 >> \theta_n$), and in the opposite situation, when it is negligible ($\theta_0 << \theta_n$). These correspond to low and high energy particles respectively.

If the MS dominates no fitting method can improve the results over that one obtained using only the two first points. In this limit, the MS ruins the tracker precision. Take for example the track slope resolution at the interaction vertex (that is at the middle of the converter) using only two planes:

$$\sigma_\theta^2 = 2\,(\frac{\sigma}{d})^2 + \frac{1}{3}\theta_0^2(\frac{z}{d})^2 + \frac{1}{2}\theta_0^2 \tag{11}$$

the first term is the slope error calculated with the two hits, the second term is the dispersion of the second hit due to the multiple scattering, the third term is extrapolation error at the vertex position. If the multiple scattering dominates, one obtains:

$$\sigma_\theta = \sqrt{\frac{1}{3}(\frac{z}{d})^2 + \frac{1}{2}}\;\;\theta_0 \tag{12}$$

It shows clearly that the foil configuration (null thickness converter $z = 0$) provides better resolution than the configuration in which the material is uniformly distributed along the planes gap ($z = d$). The resolution is limited to $\sqrt{1/2}\,\theta_0$ in the best case.

If the MS is negligible (the particle is energetic enough), the KF should (and if fact does) reach the least square fit of a straight line. The expected covariance matrix at the first plane is then:

$$C_0 = \begin{pmatrix} \frac{\sum i^2}{D}\,\sigma^2 & -\frac{\sum i}{D}\,\frac{\sigma^2}{d} \\ -\frac{\sum i}{D}\,\frac{\sigma^2}{d} & \frac{N}{D}\,(\frac{\sigma}{d})^2 \end{pmatrix} \tag{13}$$

where N is the number of planes, and $D = N\sum_{i=0}^{N-1} i^2 - (\sum_{i=0}^{N-1} i)^2$. The covariance elements depend on the nominal resolutions σ or $\theta_n = \frac{\sigma}{d}$, and dimensionless factors that

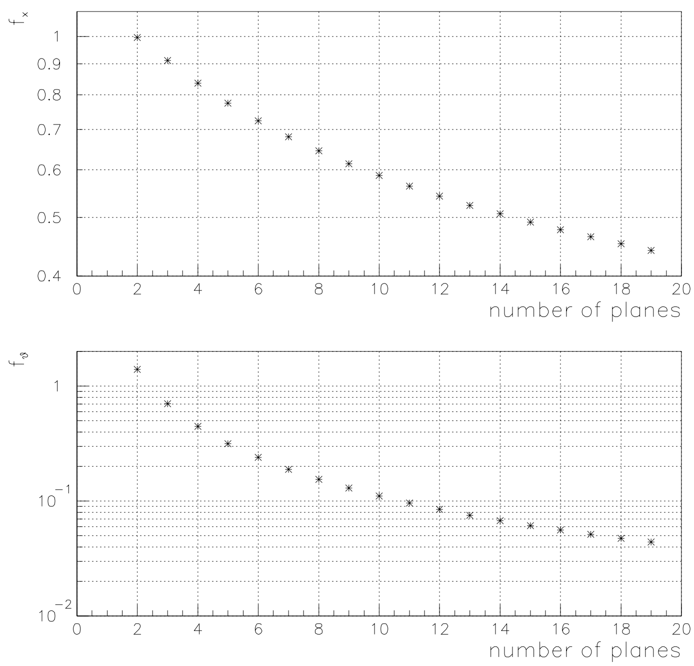

Figure 1: Improving factors (a) f_x (position) and (b) f_θ (slope) in the case of no multiple scattering.

quantify the improvement of the nominal resolution as a function of the number of planes, we call these *the improving factors*; for the track slope, e.g. $f_\theta = \sqrt{\frac{N}{D}}$. Figure 1 shows the improving factors as a function of the number of planes used in the fit.

3.4 Intermediate region

The KF provides a simple way to compute the track parameter resolution, in the intermediate region where the multiple scattering and the nominal resolution compete ($\theta_0 \sim \theta_n$). The covariance matrix at the vertex position can be computed following the KF steps:

1. The initial covariance matrix at the first measurement plane should reflect our ignorance of the track slope, for that purpose, a large number M is introduced at $\mathbf{C}_0$:

$$C_0 = \begin{pmatrix} \sigma^2 & 0 \\ 0 & M \end{pmatrix} \tag{14}$$

2. Apply the "filter" until we reach the last plane, using the equation to compute the *projected* and *fitted* covariance matrices:

$$\begin{aligned} \mathbf{C}_{k,proj} &= \mathbf{F}_{k-1}\mathbf{C}_{k-1}\mathbf{F}_{k-1}^T + \mathbf{Q}_{k-1} \\ \mathbf{C}_k &= [\mathbf{C}_{k,proj}^{-1} + \mathbf{H}^T\mathbf{G}\mathbf{H}]^{-1} \end{aligned} \tag{15}$$

3. Return to the first plane with the "smoother" procedure, and compute the *smoothed* covariance matrices, in particular, at the first plane.

$$\begin{aligned} \mathbf{A}_k &= \mathbf{C}_k\mathbf{F}_k^T\mathbf{C}_{k+1,proj}^{-1} \\ \mathbf{C}_{k,smooth} &= \mathbf{C}_k + \mathbf{A}_k(\mathbf{C}_{k+1,smooth} - \mathbf{C}_{k+1,proj})\mathbf{A}_k^T \end{aligned} \tag{16}$$

4. Extrapolate the covariance matrix to the interaction point, which is located, in average, at the middle of a converter plane, and add the covariance matrix of the multiple scattering produced in that length.

Now, the covariance matrix at the vertex $\mathbf{C}_{vertex}$ contains the track parameter resolutions.

This calculation can be done in a general way, using a dimensionless parameterization. That follows from expression (13) where the elements of the covariance matrix can be factorized in two terms: the physical factors (the nominal resolutions, σ and $\theta_n = \sigma/d$), and the dimensionless *improving factors* $f_x, f_{x\theta}, f_\theta$, that are functions of the number of planes and the multiple scattering.

$$\mathbf{C_k} = \begin{pmatrix} f_x^2\,\sigma^2 & f_{x\theta}\,\frac{\sigma^2}{d} \\ f_{x\theta}\,\frac{\sigma^2}{d} & f_\theta^2\,(\frac{\sigma}{d})^2 \end{pmatrix} \tag{17}$$

It can be demonstrated that the covariance matrix computed with two measurement planes has already the same factorization properties of (13); and that if given a plane with a covariance matrix factorized in this way, the covariance matrix at the next plane, will also have the same factorization property. In order to do that, the MS matrix has to be parameterized with two dimensionless factors, $f_{ms} = \frac{\theta_0}{\theta_n}$ and $f_z = \frac{z}{d}$. The factor f_{ms} represents the contribution of the multiple scattering error compared with the nominal resolution, (this is the important parameter that carries the MS error effect -note that $f_{ms} = \frac{d\,\theta_0}{\sigma}$, where $d\,\theta_0$ can be consider also as "the error in the position" due to the MS-); f_z is a geometrical factor, that gives the ratio of the converter to the total gap and it allows all the cases from thin foils to uniform distributed material along the gap. We apply the steps described above to the dimensionless case, the relevant matrices simplify to:

$$\mathbf{F} = \begin{pmatrix} 1 & 1 \\ 0 & 1 \end{pmatrix} \quad \mathbf{G} = \begin{pmatrix} 1 & 0 \\ 0 & 0 \end{pmatrix} \quad \mathbf{Q} = \begin{pmatrix} 1/3f_{ms}^2f_z^2 & 1/2f_{ms}^2f_z \\ 1/2f_{ms}^2f_z & f_{ms}^2 \end{pmatrix} \tag{18}$$

The computed covariance matrix at the vertex position $\mathbf{C}_{vertex}$ contains the improving factor with respect to the nominal resolutions. This parameterization allows to make a general computation, and the final parameter resolution depends (through an improving

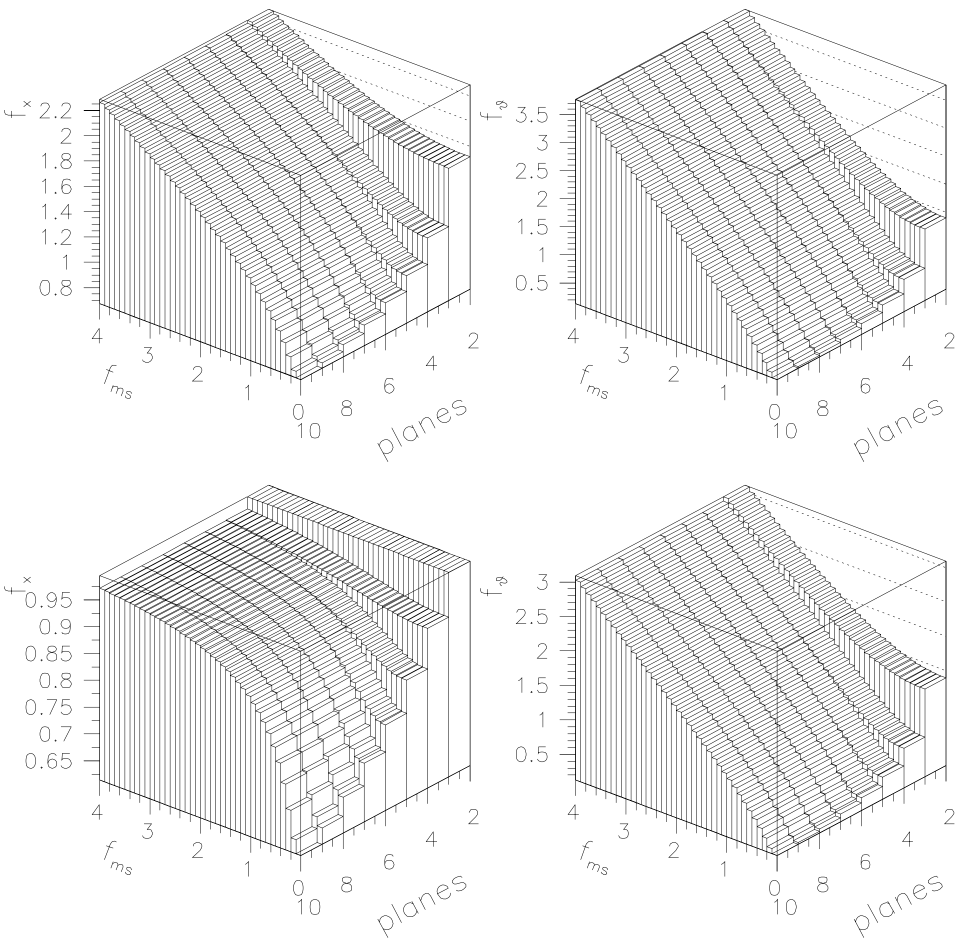

Figure 2: Improving factors for (a) f_x position and (b) f_θ track slope for the case of uniform distributed material ($f_z = 1$); and (c) f_x position and (d) f_θ track slope for the case of a thin foil converted ($f_z = 0$).

factor) on two parameters: the total number of planes N, and the ratio of the multiple scattering with respect the nominal resolution ($f_{ms} = \frac{\theta_0}{\theta_n}$).

Figure 2 shows the improving factors at the vertex position for the position and slope as a function of the number of planes N, which varies from 2 to 10, and the MS factor f_{ms}, which varies from 0 to 4. The cases considered are: the thin foil converter and the uniformly distributed material along the gap. These functions show how the MS tends to dominate quickly the resolution. If we consider for example the slope improving factor for the thin foil case (see also figure 3), already at $f_{ms} = 0.3$ the number of relevant planes is 6 and the resolution can not be improved better than a factor $f_\theta \simeq 0.3$. At $f_{ms} = 1$ only three planes gives the total information, and approximately at $f_{ms} = 2$ only two start to be relevant, and from there, it enters the asymptotic region. On the other side, only at $f_{ms} < 0.1$ the effects of large number of planes are relevant, and at $f_{ms} = 0$ the improving factor reaches the limit or no MS. The figure 3 shows the improving factor for the track slope in the case of thin material, for the case of 3, 6 and 17 planes; this is the function relevant for GLAST; if the nominal resolution is in the order of $\theta_n \sim 0.1^0$, the track slope resolution depending on the energy could vary form 3^0 to 0.01^0. The table 5 list the values of f_θ for different planes and MS factor. The figure 4 shows the improving factor for the track position at the vertex, in the case of uniform distributed material, for 3, 6 and 17 planes, this is the function relevant for NOMAD-STAR, in this case if the resolution is $\sigma = 10$ μm, the improving factor - for six planes tracker- varies from $8 - 25$ μm.

3.4.1 Dependence with the track incident angle

The track parameters degraded with increasing angles away from the normal incidence. The MS error has already been computed, and it increases proportional to $1/\cos^{5/2}\theta$. In some detectors the hit precision depends also on the incident angle of the particle, if the resolution can be expressed with a given function $\xi(\theta)$, like, $\sigma(\theta) = \xi(\theta)\ \sigma$, the above calculations are still valid, in one substitutes:

$$\sigma \to \xi\ \sigma; \quad \theta_n \to \xi\ \theta_n; \quad \theta_0 \to \frac{1}{\cos^{5/2}\theta}\ \theta_0; \quad f_{ms} \to \frac{1}{\xi\ \cos^{5/2}\theta}\ f_{ms} \tag{19}$$

We can separate the two x and y projections that are almost independent, the scaling factor is now:

$$\theta_{0,x} \to \frac{1}{\cos^2\theta_x \cos^{1/2}\theta}\ \theta_0; \quad f_{ms} \to \frac{1}{\xi \cos^2\theta_x \cos^{1/2}\theta}\ f_{ms} \tag{20}$$

for the x projection, where θ is the spatial angle. The x projected angle (θ_x) can be expressed as a function of the director cosines: $\tan\theta_x = \tan\theta\ \cos\varphi$, a similar expression is obtained for the y-projection.

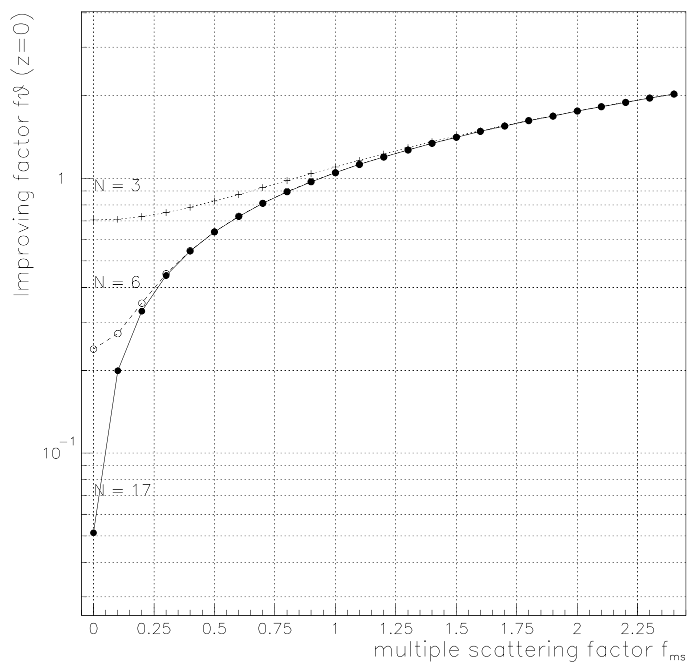

Figure 3: Slope Improving Factor (f_θ) at the vertex position for the case of thin foil converter, the curves are shown for trackers with 3, 6 and 17 planes.

4 Application to GLAST

The discussion of the previous section can be applied straight forward to the GLAST experiment; in fact, we started the calculation trying to understand how the MS error effects GLAST.

The GLAST gamma-ray telescope will investigate high energy cosmic photons and will explore high energy gamma sources in the Universe, especially AGN, Active Galactic Nuclei, with a estimated discovery probability 10^2 better than the previous experiment, EGRET [7]. GLAST is planned to be launched by NASA at 2005 and will orbit the Earth at 600 Km. One of the advantages of GLAST respect EGRET, is the precision which can locate the gamma sources with, that is, the precision of its tracker.

The basic GLAST design is made of 25 identical towers, located in a grid of 5×5. Each tower has a tracker and a calorimeter. The tracker is made of 16 modules, each one containing a converted plane of Pb with 3.5 % radiation length and two silicon detector planes with strips running in perpendicular directions and with 200 μm readout-pitch. The silicon planes and the support structure contribute with $x_0 = 0.013$ to the total

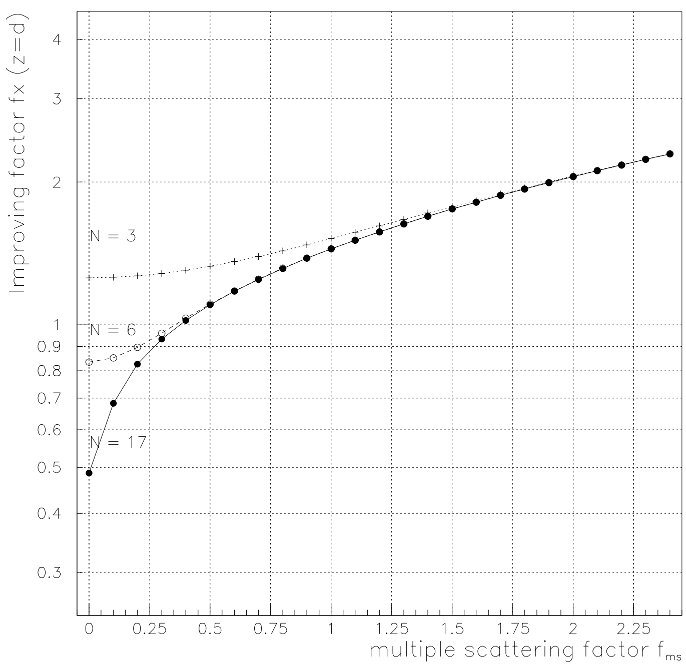

Figure 4: Position Improving Factor (f_x) at the vertex position for the case of uniform distributed material, the curves are shown for trackers with 3, 6 and 17 planes.

material. The trays are separated 3.2 cm. The photons convert, in 40% of the cases, at the passive material, in the other 60% they interact in the calorimeter. Their direction is reconstructed by tracking the resulting electron and positron. The tracker design matches the general scheme described above and the trajectories are straight lines.

The GLAST precision, compared with other kinds of telescopes, is rudimentary. Its precision has to be in the order of 3^0 and 0.4^0 for gammas between 0.1 and 1 GeV respectively. The best precision is preferred, but that forces the reduction in the thickness of the material and this compromises the number of gammas to be recorded (i.e. it degrades the *Effective Area*). The GLAST parameters have been optimized using a Monte Carlo simulation [8] . The best option chosen has 16 measuring planes, a nominal resolution of $\theta_n = 0.13^0$ and a total converter thickness $x_0 = 0.035 + 0.013$.

The relevant quantity for GLAST is the *Point Spread Function*, that is, the resolution in the initial gamma direction. In order two compute the PSF we have made the simple (crude) assumptions: 1) The gamma energy is shared between the electron and positron with equal probability, that gives on average an energetic track with 75 % of the gamma energy, and the other one with 25 %; and 2) The gamma direction resolution can be

	0.1 GeV	1 GeV	10 GeV	100 GeV
GLAST simulation	3^0	0.4^0	0.07^0	
PSF	2.44^0	0.27^0	0.048^0	0.012^0

Table 1: Comparation of the PSF obtained with the GLAST simulation [9] and with the PSF method, for normal incident angles.

derived from the combination of the two tracks directions: $\vec{p}_\gamma \simeq \vec{p}_{e^-} + \vec{p}_{e^+}$, where p is the momentum; and therefore the resolution in the slope, at least for normal incident gammas, could be approximated by: $\sigma^2_{\theta,\gamma} \simeq (\frac{E_e}{E_\gamma})^2\sigma^2_{\theta,e} + (\frac{E_{e^+}}{E_\gamma})^2\sigma^2_{\theta,e^+}$, where E is the energy. Figure 5 shows the PSF for the GLAST parameters, using these assumptions and the calculation of the previous section. The PSF is shown for different gamma incident angles. We have made the hypothesis that σ is constant, because the hit resolution can not be worse that the strip resolution where the particle enters in. We have chosen the azimuthal angle $\varphi = 45^0$ which gives the best PSF for a given incident angle θ. Note that the angular resolution (the PSF in degrees) and the slope resolution are related *via* a factor $1/\cos^2\theta$, that is, for high energy particles the slope resolution reaches *a plateau* that depends on the number of planes N=16, but the same angular resolution in degrees (PSF) improves with the angle. In the intermediate region the angular resolution compesates the extra error in multiple scattering introduced by the incident angle!. And for low energy particles, the increasing of the multiple scattering dominates (approximately with a factor $1/\cos^{1/2}\theta$). Only for angles greater that 40^0 the azimuthal angle φ starts to have some influence. This asymptotic limits agree with the naïve calculation done without the KF. Table 4 compares the results obtained with this method and the values obtained with the GLAST simulation [9]. The values are close, but consistently better than the simulated one. Especially in the intermediate region, where the multiple scattering and the nominal resolution compete. In this region we expected the largest improvement, because the present GLAST reconstruction does not use the Kalman Filter technique. The comparison shows that the computed "PSF" could be used as a first approximation to the PSF function.

If fact, we expected that this computation will be optimistic, because we did not take several considerations into account. Regarding the fit procedure, the Kalman Filter gives *optimal* parameter when the system is linear and the errors are Gaussian. The first condition is fulfill by GLAST, but not the second one. First, the multiple scattering error has important non-Gaussian tails; and second, the measurements (made by microstrip silicon detector with digital readout) only provide discrete hits (the strip positions) and the probability that the particle has passed within in the half of the pitch around the hit strip is uniform (neither of the resolutions are Gaussian). The discreteness of the measurement and its flat distribution probability should be studied with more detail to be included properly into the KF. The energy loss of the electrons has not been consider but could be implemented.

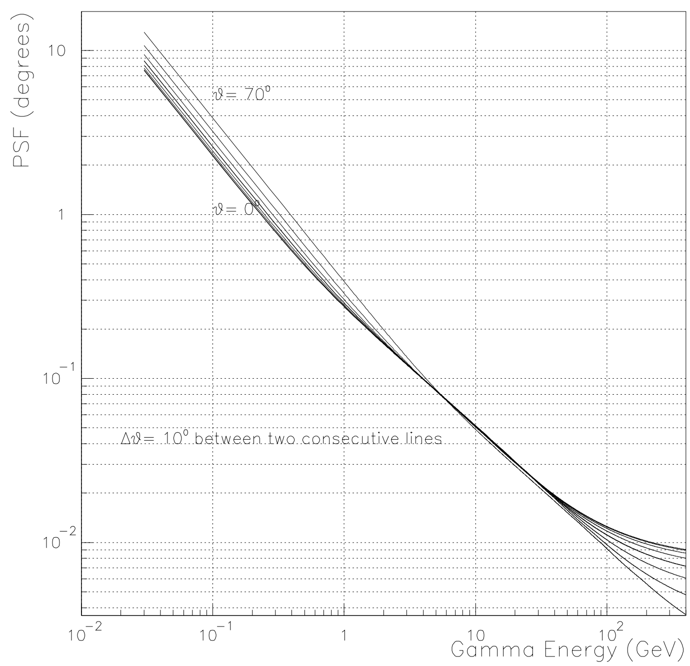

Figure 5: PSF for different indicent angles, upper line $\theta = 70^0$, lower line $\theta = 0^0$, the separation between two consecutive lines is $\Delta\theta = 10^0$. The spatial resolution has been consider constant. The azimuthal angle φ is 45^0.

And especially regarding the physics, the assumptions to compute the PSF are crude, a proper description should take into account the correct energy sharing between the electron and the positron and the recoiling of the nucleus. And also, some instrumental effects, like the pattern recognition problem (i.e in a fraction of the cases only one track will be reconstructed), the detector inefficiency, the ghost and lost hits, the dead areas, the matching with the calorimeter, and how the resolution in the energy will affect the KF and the PSF.

Finally to study the dependence with the pitch and the thickness of the converter, four energy points have been selected: E=0.1, 1, 10, 100 GeV, for a configuration with 16 planes. Figures 6 and 7 show the PSF as a function of the nominal resolution $\theta_n = \frac{pitch}{\sqrt{12}d}$ and the thickness x_0 for these energies. The contours correspond to equal resolution values. For low energy the contours are almost vertical, that is, there is no dependence with the nominal resolution, and for high energy, the contours are horizontal, that is, there is no dependence with the thickness, as expected. In the intermediate region, the relation of the pitch to the thickness is shown in the curves. To obtain the same resolution, one can decreases the nominal resolution and then one is allowed to increase the thickness, or vice-versa. The pitch is more relevant as the energy increases and it dominates the resolution above 10 GeV. A factor 2 in the pitch worsen the resolution by 2 at high energies, and little at low energies. For the thickness, the effect is the contrary, at low values, double thickness worsens the resolution by a factor $\sqrt{2}$ and its effects are almost irrelevant at high energies.

5 conclusions

We have calculated, using the Kalman Filter technique, the *improving factor* for the position and the slope, in the case of a straight line trajectory in a periodic tracker. This calculation can be done in a general way and depends on two parameters: the number of planes and the ratio between the multiple scattering slope error and the nominal slope resolution.

The application for GLAST is straight forward. With crude assumptions, one can compute a first approximation to the PSF. The PSF allows the study of the dependence with pitch, radiator thickness and incident angle. The results obtained with the PSF are close but better that the simulated ones and confirm that the optimized values for GLAST are approximately correct.

This method may be applied to different experiments with the same configuration, like NOMAD-STAR or future gamma-ray telescopes. Table 5 allows us to compute the track slope resolution at the vertex position for a given configuration, in the case of thin foil converted.

Acknowledgements

I would like to thank Bill Atwood for his encouraging support of my initial calculations, without his ideas and final comments and corrections this note will have not seen the light. Comments and suggestions from R. Johnson, W. Kröger and B. Jones were of great help, too. Special thanks to J.J. Gomez-Cadenas for the reading and correction of the first version (supposedly in English) of the note, and the help clarifying the formulas from the people of my previous experiment, NOMAD-STAR, A. Cervera-Villanueva and V.E. Kuznetsov.

References

[1] GLAST proposal to the DoE, http://www-glast.standord.edu.

[2] K.E. Kalman, J. Basic Eng. 83 (1961) 34.
K.E. Kalman and R.S. Bucy, J. Basic. Eng. 83 (1961) 95.

[3] R. Frühwirth *Application of Kalman Filtering to Track and Vertex Fitting.* Nucl. Instr. and Meth. **A 262**, (1987) 444.

[4] P Billoir. Nucl. Instr. and Meth. **A 225**, (1984) 352.

[5] B. Jones and B. Tompkins,*A Physicist's Guide to Kalman Filters* GLAST internal note. htt://www-glast.stanford.edu/protected/files/beamtest.
B. Jones and B. Tompkins, presentation at the GLAST collaboration meeting, GSFC february 1998.

[6] G. Barichello *et al. A Silicon Target for the Detection of Neutrino Interactions*. NOMAD internal note 98-004, submitted to Nucl. Instr. and Meth.
J.J. Gomez-Cadenas, J.A. Hernando, A. Bueno. Nucl. Instr. and Meth. **A 378** (1996) 196.
J.J. Gomez-Cadenas and J.A. Hernando. Nucl. Instr. and Meth **A381** (1996) 223.

[7] D.J. Thompson *et al.* ApJ Suppl, Vol 86, p629, 1993.

[8] W.B. Atwood *"Design Issues for GLAST Silicon Strip Pair Conversion Telescope"*, SCIPP 97/31, may 1997.

[9] W.B. Atwood private communication.

N	a_0	a_1	a_2	a_3	b_0	b_1
2	1.398	0.015	0.192	-0.023	0.798	0.584
3	0.669	0.119	0.351	-0.071	0.417	0.667
4	0.417	0.406	0.278	-0.072	0.418	0.668
5	0.281	0.672	0.118	-0.041	0.415	0.669
6	0.208	0.855	-0.015	-0.011	0.414	0.669
7	0.165	0.977	-0.111	0.011	0.414	0.669
8	0.137	1.062	-0.180	0.027	0.414	0.669
9	0.118	1.124	-0.233	0.039	0.414	0.669
10	0.104	1.173	-0.275	0.049	0.414	0.669
11	0.093	1.212	-0.309	0.058	0.414	0.669
12	0.084	1.245	-0.338	0.065	0.414	0.669
13	0.077	1.273	-0.362	0.072	0.414	0.669
14	0.070	1.297	-0.384	0.077	0.414	0.669
15	0.065	1.317	-0.403	0.081	0.414	0.669
16	0.060	1.335	-0.418	0.085	0.414	0.669
17	0.056	1.351	-0.433	0.089	0.414	0.669
18	0.052	1.364	-0.445	0.092	0.414	0.669
19	0.049	1.377	-0.456	0.094	0.414	0.669

Table 2: Slope improving factor f_θ at the vertex position for the case of thin foil converter. The improving factor has been fitted to a 3-degree polinomian between $f_{ms} = 0. - 2.5$, that is, in this region $f_\theta = a_0 + a_1 f_{ms} + a_2 f_{ms}^2 + a_3 f_{ms}^3$. From $f_{ms} > 2.$ the improving factor has been fitted to a straight line, that is, for this region, $f_\theta = b_0 + b_1 f_{ms}$.

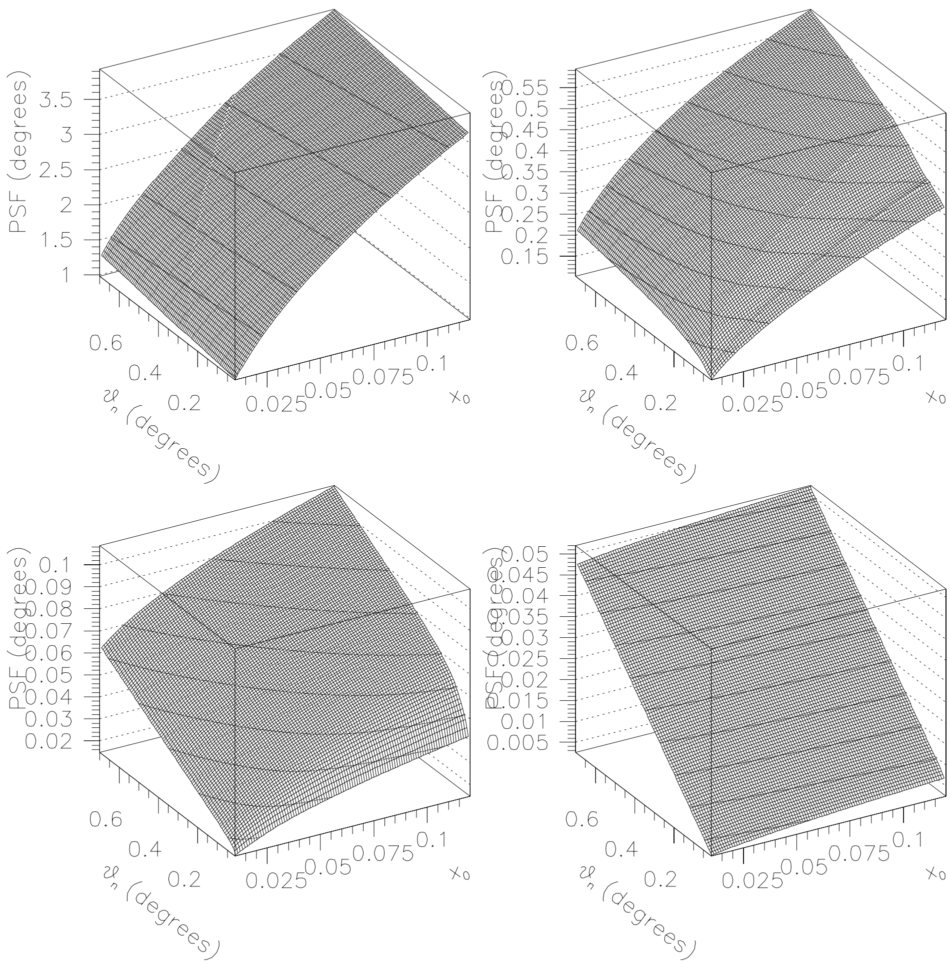

Figure 6: PSF for four different energy gammas, as a function of the nominal resolution θ_n and the thickness of the converter x_0. The energy values are (a) 0.1 GeV; (b) 1 GeV; (c) 10 GeV; (d) 100 GeV.

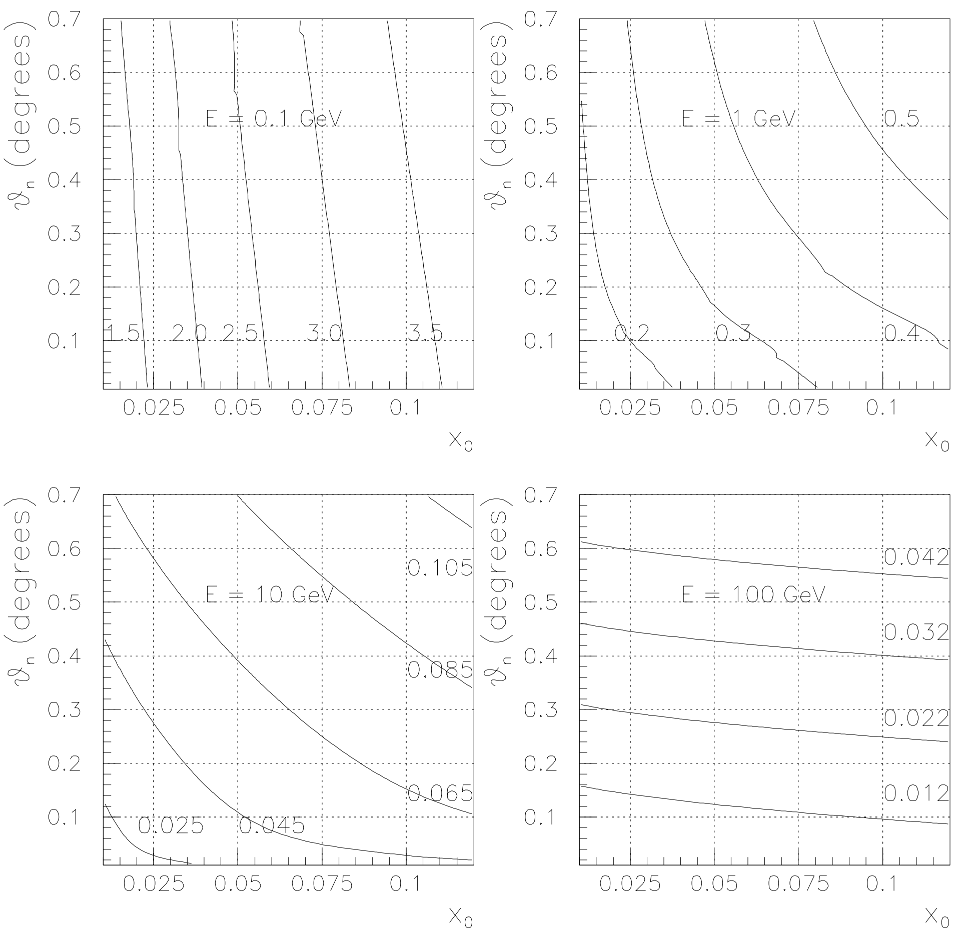

Figure 7: Contour plots of the PSF for four different energy gammas, as a function of the nominal resolution θ_n and the thickness of the converter x_0. The energy values are (a) 0.1 GeV; (b) 1 GeV; (c) 10 GeV; (d) 100 GeV. The value of the lines are the PSF in degrees.